Inorganic Chemistry

Article

pubs.acs.org/IC

Application of Mechanosynthesized Azine-Decorated Zinc(II) Metal–Organic Frameworks for Highly Efficient Removal and Extraction of Some Heavy-Metal Ions from Aqueous Samples: A Comparative Study

Elham Tahmasebi,[†] Mohammad Yaser Masoomi,[†] Yadollah Yamini, and Ali Morsali*

Department of Chemistry, Faculty of Sciences, Tarbiat Modares University, Tehran, Islamic Republic of Iran

Supporting Information

ABSTRACT: The three zinc(II) metal–organic frameworks $[Zn_2(oba)_2(4\text{-bpdb})]\cdot(DMF)_x$ (TMU-4), $[Zn(oba)(4\text{-bpdh})_{0.5}]_n\cdot(DMF)_y$ (TMU-5), and $[Zn(oba)(4\text{-bpmb})_{0.5}]_n\cdot(DMF)_z$ (TMU-6) [DMF = dimethylformamide, H_2oba = 4,4′-oxybisbenzoic acid, 4-bpdb = 1,4-bis(4-pyridyl)-2,3-diaza-1,3-butadiene, 4-bpdh = 2,5-bis(4-pyridyl)-3,4-diaza-2,4-hexadiene, and 4-bpmb = N^1,N^4-bis((pyridin-4-yl)methylene)-benzene-1,4-diamine], which contain azine-functionalized pores, have been successfully synthesized by mechanosynthesis as a convenient, rapid, low-cost, solventless, and green process. These MOFs were studied for the removal and extraction of some heavy-metal ions from aqueous samples, and the effects of the basicity and void space of these MOFs on adsorption efficiency were evaluated. The results showed that, for trace amounts of metal ions, the basicity of the N-donor ligands in the MOFs determines the adsorption efficiency of the MOFs for the metal ions. In contrast, at high concentrations of metal ions, the void space of the MOFs plays a main role in the adsorption process. The studies conducted revealed that, among the three MOFs, TMU-6 had a lower adsorption efficiency for metal ions than the other two MOFs. This result can be attributed to the greater basicity of the azine groups on the TMU-4 and TMU-5 pore walls as compared to the imine groups on the N-donor ligands on the TMU-6 pore walls. Subsequently, TMU-5 was chosen as an efficient sorbent for the extraction and preconcentration of trace amounts of some heavy-metal ions including Cd(II), Co(II), Cr(III), Cu(II), and Pb(II), followed by their determination by flow injection inductively coupled plasma optical emission spectrometry. Several variables affecting the extraction efficiency of the analytes were investigated and optimized. The optimized methodology exhibits a good linearity between 0.05 and 100 $\mu g\ L^{-1}$ ($R^2 > 0.9935$) and detection limits in the range of 0.01–1.0 $\mu g\ L^{-1}$. The method has enhancement factors between 42 and 225 and relative standard deviations (RSDs) of 2.9–6.2%. Subsequently, the potential applicability of the proposed method was evaluated for the extraction and determination of target metal ions in some environmental water samples.

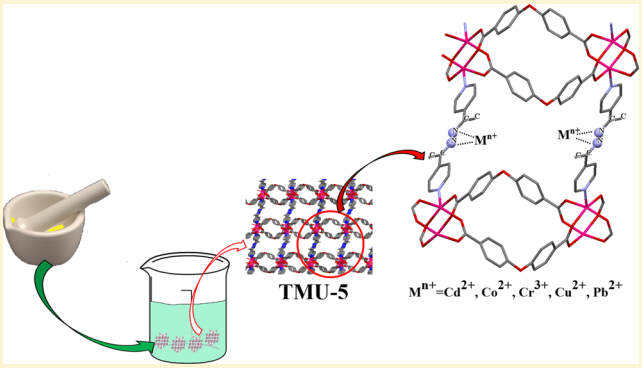

INTRODUCTION

Metal–organic frameworks (MOFs), as a new class of crystalline porous materials, have received great attention in the past decade because of their intriguing structures.[1] The unique characteristics of MOFs include high surface area, good thermal stability, uniform structured nanoscale cavities, uniform but tunable pore size, controllable particle dimensions and morphology, accessible cages and tunnels, specific adsorption affinities, and the availability of in-pore functionality and outer-surface modification.[2] These features make MOFs very promising materials for recognition,[3,4] separation,[5−7] gas storage,[8−10] sensing,[11] drug delivery,[12,13] biomedical imaging,[14] and catalysis.[15−17] The diverse structures and unique properties also make MOFs attractive for analytical applications.[18] MOFs have been successfully explored as sorbents for sampling,[19,20] solid-phase extraction (SPE),[21,22] and solid-phase microextraction[23−25] and as stationary phases for gas chromatography[26−30] and liquid chromatography.[31−36] However, the exploration of MOFs as efficient sorbents for sample preparation is still controversial. Indeed, problems can arise in the application of MOFs as sorbents in aqueous matrixes or in their exposure to even very small amounts of moisture. Water stability is a key property for MOFs in many applications, especially in sample preparation techniques, as most biological and environmental samples contain water. However, few efforts have been made in this area.

Heavy metals as persistent environmental contaminants are of great importance among chemical pollutants. Potential sources of heavy-metal-ion pollution include various effluents

Received: July 2, 2014
Published: December 30, 2014

DOI: 10.1021/ic5015384
Inorg. Chem. 2015, 54, 425−433

emanating from industrial facilities, domestic activities, and erosion of natural deposits. Recently, the toxicity and effects of trace elements that are dangerous to public health and the environment have attracted increasing attention in the fields of pollution and nutrition.[37] At trace levels, several heavy metals such as chromium, copper, and cobalt are essential micronutrients for plants, living organisms, and the human body, whereas in large amounts, the same elements are toxic. On the other hand, lead and cadmium are well-recognized to be highly toxic and hazardous to human health even at low concentrations.[37] As a consequence, contamination levels in urban and industrial wastewaters need to be controlled, and strict regulations have been drawn up and proposed in this regard. Accordingly, the removal and determination of heavy metals in different samples is desired, and achieving a fast, simple, sensitive, and accurate method of analysis is necessary. In various publications, different analytical methods have been reported for the determination of metal ions, such as flame or electrothermal atomic absorption spectroscopy (FAAS or ETAAS, respectively), inductively coupled plasma optical emission spectrometry (ICP-OES), and inductively coupled plasma mass spectrometry (ICP-MS).[38−40]

Because of the low concentrations of metal ions and the high number of interfering species present in complicated matrixes, the direct determination of such ions at trace levels is limited. Therefore, a sample preparation step prior to final analysis is intended to improve the sensitivity and accuracy of the assay by removing the majority of the matrix interference while concentrating the analyte. Among sample preparation techniques, solid-phase extraction (SPE) has become well-established for preconcentrating the desired components from a sample matrix because of its many obvious advantages, such as high extraction efficiency, low consumption of organic solvents, rapidity, and convenience of operation.[41] Given that, in the SPE procedure, the sorbent plays a very prominent role in the analytical performance (i.e., analytical sensitivity, selectivity, and precision), most of the current studies on SPE focus on the development of new sorbents.

In our previous study, the two Zn(II)-based MOFs $[Zn_2(oba)_2(4\text{-bpdb})]_n\cdot(DMF)_x$ (TMU-4) and $[Zn(oba)(4\text{-bpdh})_{0.5}]_n\cdot(DMF)_y$ (TMU-5) [DMF = dimethylformamide, H_2oba = 4,4-oxybisbenzoic acid, 4-bpdb = 1,4-bis(4-pyridyl)-2,3-diaza-1,3-butadiene, and 4-bpdh = 2,5-bis(4-pyridyl)-3,4-diaza-2,4-hexadiene; Scheme 1] were successfully synthesized by mechanosynthesis for the first time, and their CO_2 adsorption properties were investigated.[42] The studies conducted demonstrated that the azine decoration of the pore surfaces in TMU-4 and TMU-5 plays a significant role in CO_2 uptake because of the Lewis basic property of the azine groups on the pore surface and their moderately strong interactions with CO_2. Considering that the N-donor ligands contain a bridging azine group in the middle (Scheme 1), we intended to assay the Lewis basic features of azine groups on the pores wall of TMU-4 and TMU-5 toward the adsorption of metal ions in further studies. For further investigation regarding the role of the azine groups in capturing metal ions, another mechanosynthesized Zn(II)-based MOF, $[Zn(oba)(4\text{-bpmb})_{0.5}]_n\cdot(DMF)_z$ [TMU-6, 4-bpmb = N^1,N^4-bis((pyridin-4-yl)-methylene)benzene-1,4-diamine; Scheme 1] was selected[43] in which the introduction of a phenyl ring into the pillar ligand creates two imine groups instead of an azine group. This change helped us examine the basicity of the N-donor ligand to compare the adsorption efficiencies of the three MOFs. In addition, the metal ion adsorption capacities of the three MOFs were evaluated and compared.

In subsequent studies, the applicability of TMU-5 for the extraction and preconcentration of trace amounts of some heavy-metal ions including Cd(II), Co(II), Cr(III), Cu(II), and Pb(II) from aqueous samples, followed by their determination by flow-injection inductively coupled plasma optical emission spectrometry (ICP-OES), was investigated, and potential parameters affecting the performance of target metal ion extraction were evaluated in detail. Finally, the proposed method was applied for the preconcentration and determination of target metal ions in real environmental water samples.

Scheme 1. Chemical Structures of H_2oba, 4-bpdh, 4-bpdb, and 4-bpmb

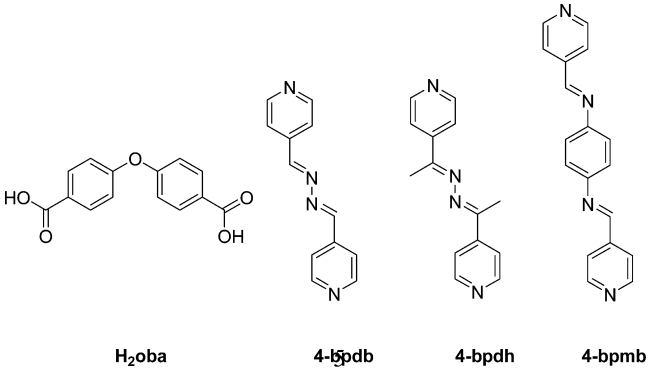

EXPERIMENTAL SECTION

Materials and Physical Techniques. Zinc(II) nitrate hexahydrate, zinc(II) acetate dihydrate, and 4,4′-oxybis(benzoic acid) (H_2oba) were purchased from Aldrich and Merck and used as received. The ligands 1,4-bis(4-pyridyl)-2,3-diaza-1,3-butadiene (4-bpdb), 2,5-bis(4-pyridyl)-3,4-diaza-2,4-hexadiene (4-bpdh), and N^1,N^4-bis((pyridin-4-yl)methylene)benzene-1,4-diamine (4-bpmb) were synthesized according to previously reported methods.[44] Unless otherwise stated, all chemicals and reagents used were of at least analytical grade and were used as received without further purification. Stock standard solutions (1000 mg L^{-1}) of Cd(II), Co(II), Cr(III), Cu(II), and Pb(II) were prepared by dissolving appropriate amounts of analytical-grade $Cd(NO_3)_2\cdot4H_2O$, $Co(NO_3)_2\cdot6H_2O$, $Cr(NO_3)_3\cdot9H_2O$, $Cu(NO_3)_2\cdot3H_2O$, and $Pb(NO_3)_2$ salts, respectively, from Merck in ultrapure water. Working standard solutions were prepared daily by diluting the stock standard solutions to the required concentrations with water purified on an Aqua Max-Ultra Youngling ultrapure water purification system (Dongan-gu, South Korea).

Natural water samples including river water (Iran), tap water (Tarbiat Modares University, Tehran, Iran), and bottled mineral water available on the market were obtained to be tested as real samples. Before analysis, the water samples were filtered through 0.45-μm cellulose acetate membranes (Millipore) and stored in brown bottles at 4 °C in a refrigerator.

Apparatus. Melting points were measured on an Electrothermal 9100 apparatus. IR spectra were recorded using a Thermo Scientific Nicolet IR100 (Madison, WI) Fourier-transform infrared (FT-IR) spectrometer. The thermal behavior was measured on a PL-STA 1500 apparatus at a rate of 10 °C min^{-1} in a static atmosphere of argon. Powder X-ray diffraction (PXRD) measurements were performed using a Philips X'pert diffractometer with monochromated Cu Kα radiation. The samples were characterized by field-emission scanning electron microscopy (FE-SEM) on a Zeiss SIGMA VP instrument (Oberkochen, Germany) with a gold coating. Sorption studies on TMU-6 were performed using an AutosorbIQ apparatus from

DOI: 10.1021/ic5015384
Inorg. Chem. 2015, 54, 425−433

Quantachrome Instruments: CO_2 at 195 K and N_2 at 77 K. The sample was outgased at 140 °C for 12 h under a vacuum.

Simultaneous inductively coupled plasma optical emission spectrometry (ICP-OES) on a Varian Vista-PRO instrument (Springvale, Australia) with a radial torch coupled to a concentric nebulizer and a Scott spray chamber and equipped with a charge-coupled detector (CCD) was used for simultaneous determination of the target elements. A six-port two-position injection valve from Tehran University (Tehran, Iran) equipped with a 250 μL injection loop constructed from silicon tubing was used to introduce the final solution into the ICP-OES nebulizer. Table S1 in the Supporting Information (SI) lists the optimal instrumental conditions and the emission lines employed for the determination of the metal ions by ICP-OES.

Synthesis of TMU-4, TMU-5, and TMU-6. $[Zn_2(oba)_2(4\text{-bpdb})]_n\cdot(DMF)_2$ (TMU-4), $[Zn(oba)(4\text{-bpdh})_{0.5}]_n\cdot(DMF)_{1.5}$ (TMU-5), and $[Zn(oba)(4\text{-bpmb})_{0.5}]_n\cdot(DMF)_{1.5}$ (TMU-6) were synthesized according previously reported methods,[42,43] and in the mechanosynthesis procedure, the resulting powders were washed with a solution containing 15 mL of 0.05 M NaOH and 3 mL of ethanol instead of DMF to remove any unreacted starting material and then dried at 100 °C.

Extraction Procedure. The procedure for the solid-phase extraction of target metal ions was according to the following steps:

A 200 mL aliquot of an aqueous sample containing the target analytes, adjusted to pH 10, was placed in a 250 mL glass beaker. Then, 7 mg of the sorbent was activated with 0.05 mL of methanol and 2 mL of distilled water under a fierce vortex and added to the sample solution. The solution was stirred gently for 5 min using a magnetic stirrer at a constant rate of 800 rpm to facilitate adsorption of the analytes onto the sorbent. At the end of the extraction time, the solution was transferred to conical tubes and centrifuged. After decantation of the residual solution, the adsorbed target analytes were desorbed from the sorbent with 500 μL of eluent containing 0.4 M ethylenediaminetetraacetic acid (EDTA) by fierce vortex for 5 min. Then, the eluate was isolated from the mixture by centrifugation, and 250 μL of this solution was introduced into the nebulizer of the ICP-OES instrument using the six-way two-position injection valve for subsequent analysis.

To investigate the metal ion adsorption at high concentrations, 3 mg of MOF was added to 10 mL of metal ion solution at pH 6 and stirred for 15 min at a constant temperature of 27 °C. Once equilibrium was thought to have been reached, the sorbent was separated by centrifugation, and the concentrations of the residual ions in the solution after equilibrium adsorption were determined by ICP-OES.

RESULTS AND DISCUSSION

Characterization of the MOFs. In a typical synthesis, TMU-4, TMU-5, and TMU-6 were prepared by the mechanochemical reaction (grinding by hand) of a mixture of $Zn(OAc)_2\cdot2H_2O$, H_2oba, and N-donor ligand (4-bpdb, 4-bpdh, and 4-bpmb, respectively) for 15 min (Figure S1, SI). Comparison between the simulated and experimental (resulting from the mechanosynthesized powder) powder X-ray diffraction (PXRD) patterns revealed that the mechanosynthesized TMU-4, TMU-5, and TMU-6 were structurally identical to TMU-4, TMU-5, and TMU-6 prepared by conventional heating (Figure 1).

In MOF $[Zn_2(oba)_2(4\text{-bpdb})]_n\cdot(DMF)_x$ (TMU-4), a three-dimensional honeycomb framework with double interpenetration was obtained by coordination of the oba and 4-bpdb ligands to Zn(II) nodes. TMU-4 has one-dimensional open channels (aperture size of 5.3 × 9 Å, taking into account the van der Waals radii; 40% void space per unit cell)[45] running along the [101] direction in which the internal surface is decorated by the azine groups of the 4-bpdb ligands (Figure 2a, shown in blue).[42] MOF $[Zn(oba)(4\text{-bpdh})_{0.5}]_n\cdot(DMF)_y$ (TMU-5) shows narrow, three-dimensional interconnected pores (aperture size of 4.4 × 6.2 Å, taking into account the van der Waals radii; 34.6% void space per unit cell)[45] that are also functionalized with azine groups (Figure 2b, shown in blue).

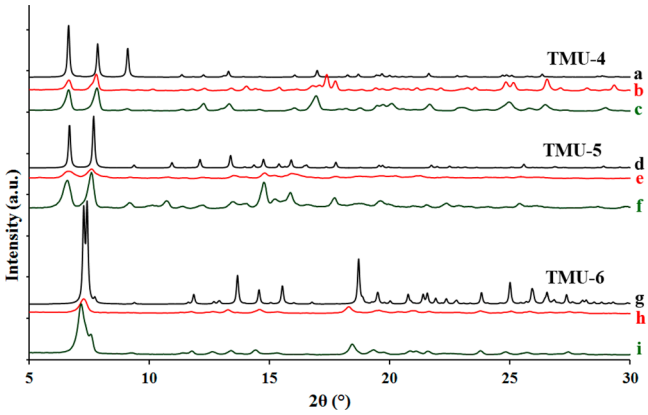

Figure 1. Comparison of PXRD patterns of TMU-4, TMU-5, and TMU-6: (a,d,g) simulated, (b,c,e,f,h,i) mechanosynthesized (b,e,h) before washing and (c,f,i) after washing with a solution containing 15 mL of 0.05 M NaOH and 3 mL of ethanol and before heating of the materials.

The structure of $[Zn(oba)(4\text{-bpmb})_{0.5}]_n\cdot(DMF)_z$ (TMU-6) is similar to that of TMU-4 but different from that of TMU-5. This can be attributed to the introduction of phenyl rings into the pillar ligand of TMU-4. In TMU-6, the Zn(II) centers are coordinated to four carboxylate O atoms from three oba ligands and one N atom from the 4-bpmb ligand. Three consecutive Zn(II) centers from two different units are connected to each other through the dicarboxylate oba ligand and the resulting two-dimensional sheets. A 3-fold interpenetrated structure is obtained by connecting these two-dimensional sheets through the linear 4-bpmb. TMU-6 has large one-dimensional pore channels running along the [101] direction (aperture size of 9.1 × 8.9 Å, taking into account the van der Waals radii; 34.2% void space per unit cell)[45] that are decorated with nitrogen atoms (Figure 2c).[43] Similarly to the previously reported TMU-4,[42] the mechanosynthesized TMU-6 is nonporous toward N_2 at 77 K and 1 bar (Figure S2, SI). Interestingly, TMU-6 is porous to CO_2 at 195 K and 1 bar [120.66 cm^3/g at 1 bar; Brunauer–Emmett–Teller (BET) surface area of 456 m^2/g] (Figure 3).

The TGA curves of mechanosynthesized TMU-4, TMU-5, and TMU-6 show a plateau in the range of 30–310, 30–290, and 30–380 °C respectively, revealing that their pore channels were devoid of any guest molecules (Figure S3, SI). Above these temperatures, the MOFs started to decompose.

Water Stability Tests of TMU-4, TMU-5, and TMU-6. The as-synthesized TMU-4, TMU-5, and TMU-6 were soaked in water for 12 h to determine whether they are stable in water. The PXRD patterns before and after immersion were consistent, confirming that the structures have high stabilities in water (Figure 4).

Optimization of Extraction Parameters. As the primary experiments showed that TMU-6 has a lower extraction efficiency for metal ions than the other two MOFs, TMU-5 was selected as the sorbent for extraction and preconcentration studies in subsequent experiments. To obtain the highest extraction efficiency and preconcentration factor, several experimental parameters affecting the performance of the method, such as type of eluent, sample pH, times of adsorption

DOI: 10.1021/ic5015384
Inorg. Chem. 2015, 54, 425–433

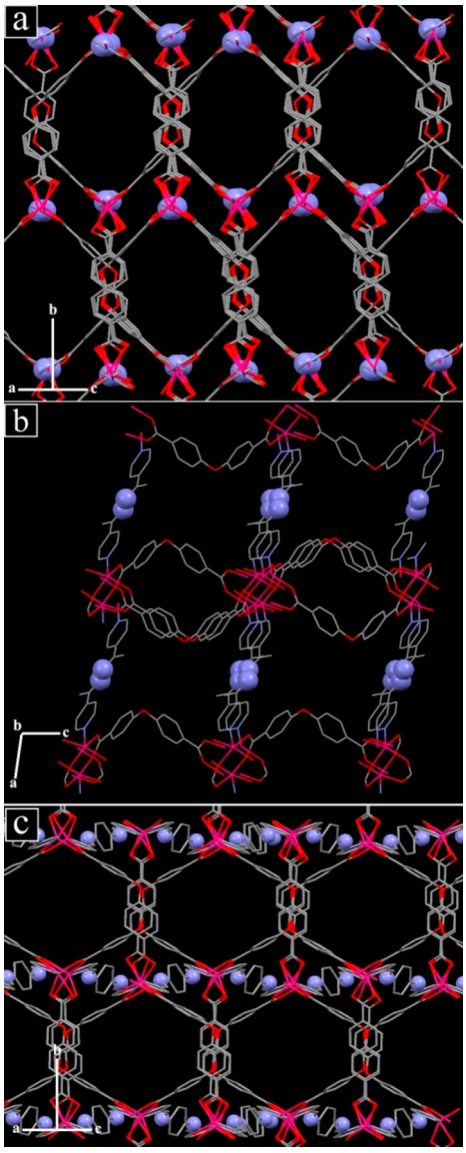

Figure 2. Representation of the pores of (a) TMU-4, (b) TMU-5, and (c) TMU-6, highlighting the azine groups (in blue). Hydrogen atoms and DMF molecules are omitted for clarity.

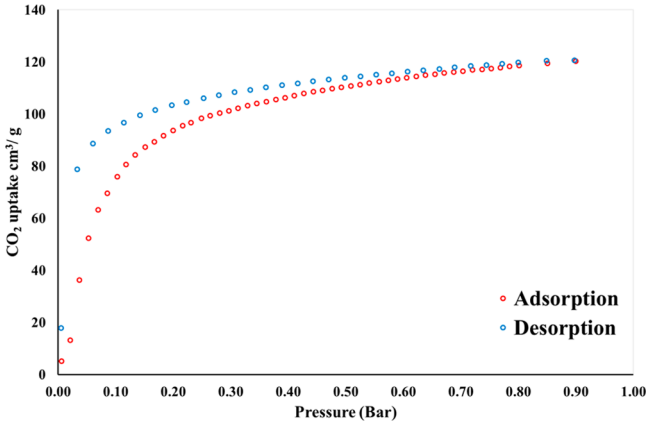

Figure 3. CO_2 isotherm at 195 K and 1 bar of mechanosynthesized TMU-6.

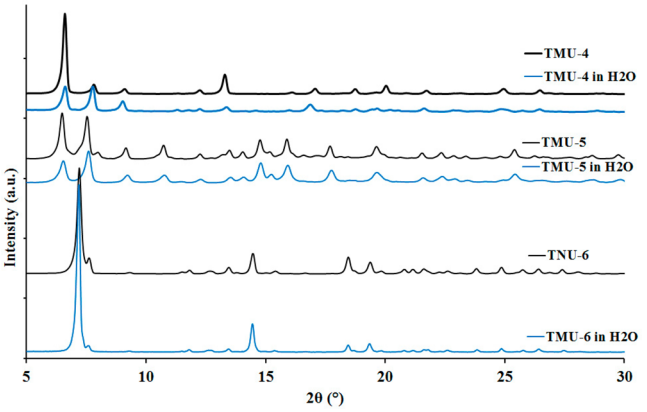

Figure 4. Comparison of PXRD patterns of TMU-4, TMU-5, and TMU-6 before and after immersion in H_2O for 12 h.

and desorption, and sample and eluent volumes, were investigated by the proposed procedure using the one-variable-at-a-time (OVAT) method. All experiments were performed in triplicate, and their averages were used as analytical signals.

Selection of the most effective eluent for the quantitative stripping of the retained target metal ions onto the sorbent is of special interest. For this purpose, to achieve more efficient desorption of target analytes from the sorbent and higher desorption recoveries, different eluents including different concentrations of HNO_3 and EDTA solutions were evaluated. As can be seen from Figure 5, 0.1 M HNO_3 solution and 0.4 M

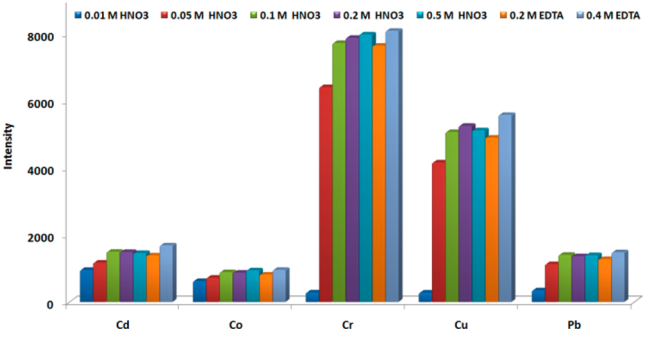

Figure 5. Effect of eluent type on extraction efficiency. Extraction conditions: sample solution, 30 mL of 100 μg L^{-1} target metal ions at pH 7; MOF, 7 mg; eluent, 200 μL; extraction time, 2 min; desorption time, 1 min. (For better viewing, the signals for Cd, Co, and Pb have been increased by 10, 10, and 5 fold, respectively.)

EDTA provided suitable desorption of the target metal ions, but because 0.4 M EDTA exhibited a better desorption efficiency, it was finally chosen as the elution solvent in the subsequent experiments.

The pH of the sample solution plays a significant role in the adsorption of target metal ions onto sorbents by affecting both the chemistry of the target metal ions in solution and the protonation of the sorbent donor atoms. Sample pH was varied in the range from 4 to 11 to investigate its effect, and the obtained results are shown in Figure 6. As can be seen, the extraction efficiency increased dramatically as the pH was increased from 4 to 10 and then decreased. This effect can be related to the protonation of sorbent donor atoms at low pH values and the formation and precipitation of hydroxide species of target metal ions at high pH values (pH > 10), leading to a

DOI: 10.1021/ic5015384
Inorg. Chem. 2015, 54, 425−433

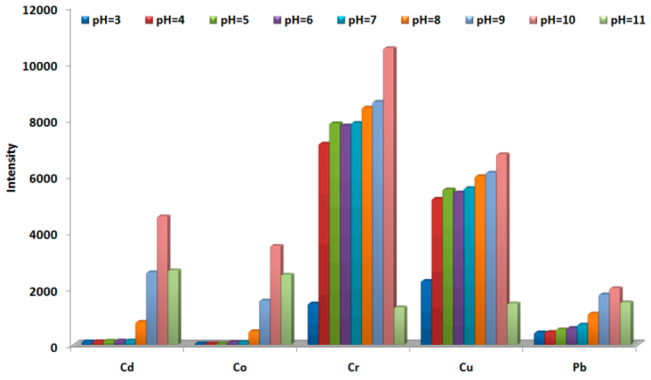

Figure 6. Effect of sample pH on extraction efficiency. Extraction conditions: sample solution, 30 mL of 100 μg L^{-1} target metal ions; MOF, 7 mg; eluent, 200 μL of 0.4 M EDTA; extraction time, 2 min; desorption time, 1 min. (For better viewing, the signal for Pb has been tripled.)

decrease in the adsorption of metal ions. According to these results, the pH of the sample solution was adjusted at pH 10 for subsequent experiments.

The effect of the sorbent amount on the adsorption efficiency of the target analytes was examined as well; for this purpose, 7−22 mg of MOF was added to the sample, and the effects of varying amounts were investigated. According to Figure 7, there was no distinct increase in extraction efficiency

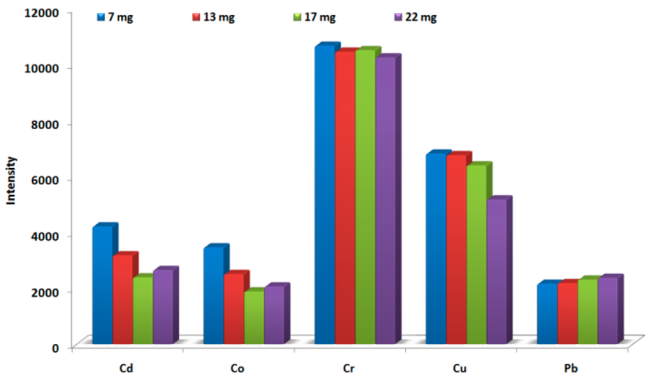

Figure 7. Effect of MOF amount on extraction efficiency. Extraction conditions: sample solution, 30 mL of 100 μg L^{-1} target metal ions at pH 10; eluent, 200 μL of 0.4 M EDTA; extraction time, 2 min; desorption time, 1 min. (For better viewing, the signal for Pb has been quadrupled.)

with increasing MOF amount, and the amount of adsorbent had a low effect on the extraction efficiency of the metal ions. This observation can be attributed to the large porosity and surface area of the MOFs, as well as the accessibility of many free coordination sites on the MOF. In addition, the azine groups on the pore surface of the MOF can have appropriate interactions with the target metal ions and provide high adsorption efficiencies. In comparison with traditional SPE sorbents, satisfactory results could be achieved using lower amounts of MOF sorbent. The decrease in the extraction efficiency with further increasing sorbent amount was due to the weak elution of the adsorbed analytes by a fixed volume of eluent. Based on these results, a sorbent amount of 7 mg was applied in further experiments.

Also, the effect of time on the extraction efficiencies was investigated in the range of 2−20 min. The obtained results are shown in Figure S4 (SI). As illustrated in this figure, the extraction efficiencies of the analytes increased as the extraction time increased from 2 to 5 min, and after that, a low decrease was observed in the signal intensity. According to this result, the extraction time had no significant influence on the extraction efficiency, and equilibrium was accomplished in 5 min, so a time of 5 min was selected as the optimum adsorption time. MOFs have very high porosities and surface areas and short diffusion routes, resulting in very rapid adsorption processes.

Further experiments were also conducted to investigate the effect of eluent volume to achieve the highest enrichment and best recovery of the adsorbed analytes. For this purpose, various eluent volumes ranging from 200 to 500 μL were studied. As demonstrated in Figure S5 (SI), the extraction recoveries reached a maximum at 500 μL of eluent; thus, 500 μL of 0.4 M EDTA solution was employed for quantitative desorption of the analytes in subsequent experiments.

The effect of desorption time on extraction efficiency was also assayed in the range of 2−10 min. The experimental results also indicated that desorption for 5 min enabled quantitative stripping of the adsorbed analytes from the sorbent, and no substantial effect was observed with additional desorption time.

In this work, to achieve better extraction efficiencies and higher preconcentration factors, the effect of the sample volume was studied using different sample volumes ranging from 30 to 300 mL of aqueous samples that were spiked with 3 μg of the target analytes in the presence of a constant amount (7 mg) of sorbent. The results indicated that the extraction efficiencies were constant up to 200 mL and subsequently decreased with further increasing the sample solution volume. Therefore, 200 mL was deemed to be the optimum sample volume.

Effect of Potentially Interfering Elements. The potential interference of some foreign ions in the preconcentration and determination of our target metal ions was examined. For this purpose, solutions containing 50 μg L^{-1} target metal ions and different concentrations of foreign ions were prepared and treated according to the optimized extraction procedure. In this study, the tolerance limits of the coexisting ions, defined as the largest amounts of the coexisting ions changing the recovery of the target metal ions by as much as ±10%, were determined and are reported in Table S2 (SI). The results demonstrated that the presence of large amounts of species commonly present in water samples has no significant effect on the extraction efficiency of the target analytes. On the other hand, the concentrations of the studied metal ions found in natural water samples are usually lower than the tolerance limits reported for them.

Evaluation of the Method Performance. To evaluate the practical applicability of the proposed extraction method, a number of performance parameters were investigated as figures of merit for the extraction of target metal ions from aqueous solutions under the optimum conditions and are summarized in Table 1. Calibration curves were constructed using 10 different concentrations of the metal ions in the range of 0.05−100 μg L^{-1}. All analytes exhibited good linearity in the studied range, with coefficients of determination ranging from 0.9935 to 0.9987. The preconcentration factors (PF), calculated as the ratios of the slopes of the calibration curves obtained by the proposed method and through the direct injection of metal ion standards into the ICP-OES system, were found to be in the range of 42−225. The extraction recoveries (ER, %) of the method were obtained in the range of 10−56%. The precision

DOI: 10.1021/ic5015384
Inorg. Chem. 2015, 54, 425−433

Table 1. Analytical Performance of the Proposed Method for the Extraction and Determination of Target Metal Ions

	linearity					precision
analyte	LDR[a] (μg L^{-1})	R^2	LOD[b] (μg L^{-1})	PF[c]	ER (%)	RSD[d] (%) (n = 4)
Cd^{2+}	0.30−100	0.9975	0.10	81	21	4.9
Co^{2+}	0.30−100	0.9982	0.10	42	10	4.3
Cr^{3+}	0.05−100	0.9987	0.01	216	54	2.9
Cu^{2+}	0.05−100	0.9981	0.02	225	56	3.2
Pb^{2+}	2.00−100	0.9935	0.50	137	35	6.2

[a]Linear dynamic range. [b]Limit of detection. [c]Preconcentration factor. [d]Data were calculated based on the extraction of a 30 μg L^{-1} sample for each analyte.

of the method, expressed as the relative standard deviation (RSD, %), were calculated by carrying out four replicate extractions and determinations of all analytes at a concentration level of 30 μg L^{-1} during 1 day, and were between 2.9% and 6.2%, showing the good repeatability of the method. ER was calculated according to the equation

$$\mathrm{ER}\ (\%) = \left(\frac{C_f V_f}{C_0 V_0}\right) \times 100$$

where C_0 and C_f denote the initial concentration of the analyte in the sample solution and concentration of the analyte in the eluate after extraction with the proposed method, respectively, and V_0 and V_f are the volumes of the sample and the eluent, respectively.

Application to Real Samples. To evaluate the reliability and analytical applicability of the suggested method in the case of real samples with different matrixes, the optimized method was applied for the determination of target metal ions in some real samples including tap water, river water, and mineral water. To reduce the matrix effect, river water and mineral water samples were diluted 2- and 1-fold, respectively, with deionized water prior to analysis. The results are reported in Table 2. Some of the target metal ions were detected in the analyzed real water samples. The accuracy of the method was verified by performing relative recovery studies in the real samples under optimum conditions. The water samples were spiked with the analytes at two levels, and relative recoveries were calculated. As can be seen, satisfactory recoveries ranging from 90 to 110% with good repeatabilities were achieved for analyzed real samples.

Comparison of Adsorption Efficiencies of TMU-4, TMU-5, and TMU-6. For better evaluation of the adsorption behavior of TMU-5 for heavy-metal ions and the role of azine groups in ion capture by TMU-5, we decided to perform further studies by comparing the adsorption efficiency of TMU-5 with that of another MOF that has free N atoms in pores surface but not azine groups. For this purpose, the new MOF TMU-6 was designed and synthesized under the same conditions. After structural analysis, which confirmed presence of free nitrogen sites on the pore walls, the extraction efficiencies of TMU-5 and TMU-6 were investigated and compared. Moreover, to evaluate the effects of the structure and pore size of MOFs on capturing the metal ions, the extraction efficiency of TMU-5 was compared to that of TMU-4.The investigations performed illustrated that the maximum extraction efficiency of the target metal ions was achieved at pH 10 for all three MOFs. Taking this fact into account, a comparison of the extraction efficiencies of these three MOFs was performed at pH 10. According to the results reported in Table 3, the extraction efficiency [stated as extraction recovery (ER)] of TMU-4 was nearly the same as that of TMU-5, whereas the extraction efficiency of TMU-6 was much less than that of TMU-5. Because TMU-5 and TMU-4 have azine groups with different structures and pore sizes and TMU-6 has a different N-donor group (there is a phenyl group between two nitrogen atoms), it can be concluded that the structure and pore size of the MOF do not have significant effects on the

Table 2. Results of the Determination of Target Analytes by the Proposed Method in Different Real Water Samples

analyte	$C_{initial}$ ± SD (μg L^{-1})	C_{added} (μg L^{-1})	C_{found} ± SD (μg L^{-1})	relative recovery (%)
		Tap Water		
Cd^{2+}	<LOD	1.0	$0.9_4 \pm 0.0_4$	94
		5.0	$5.1_9 \pm 0.3_3$	104
Co^{2+}	$0.4_1 \pm 0.0_3$	1.0	$1.3_2 \pm 0.0_8$	91
		5.0	$5.7_5 \pm 0.4_1$	107
Cr^{3+}	$0.2_5 \pm 0.0_1$	1.0	$1.2_1 \pm 0.0_5$	96
		5.0	$5.1_1 \pm 0.2_4$	97
Cu^{2+}	$0.3_1 \pm 0.0_1$	1.0	$1.2_5 \pm 0.0_9$	94
		5.0	$4.8_8 \pm 0.1_9$	91
Pb^{2+}	<LOD	2.0	$2.0_8 \pm 0.1_5$	104
		5.0	$5.4_2 \pm 0.3_1$	108
		Mineral Water[a]		
Cd^{2+}	<LOD	1.0	$1.0_8 \pm 0.0_7$	108
		4.0	$4.2_8 \pm 0.2_9$	107
Co^{2+}	$1.6_3 \pm 0.0_9$	1.0	$2.6_8 \pm 0.1_2$	105
		4.0	$5.9_3 \pm 0.3_2$	108
Cr^{3+}	$0.3_2 \pm 0.0_1$	1.0	$1.3_7 \pm 0.0_5$	105
		4.0	$3.9_8 \pm 0.1_5$	92
Cu^{2+}	$2.3_8 \pm 0.1_1$	1.0	$3.4_8 \pm 0.1_9$	110
		4.0	$6.7_0 \pm 0.2_3$	108
Pb^{2+}	<LOD	2.0	$2.0_7 \pm 0.1_7$	104
		4.0	$3.6_1 \pm 0.2_9$	90
		River Water[a]		
Cd^{2+}	$0.3_1 \pm 0.0_3$	2.0	$2.1_6 \pm 0.1_3$	93
		4.0	$3.9_3 \pm 0.2_9$	91
Co^{2+}	$0.5_1 \pm 0.0_4$	2.0	$2.5_8 \pm 0.1_8$	104
		4.0	$4.8_9 \pm 0.2_5$	110
Cr^{3+}	$0.3_3 \pm 0.0_2$	2.0	$2.4_2 \pm 0.1_0$	105
		4.0	$4.5_8 \pm 0.1_8$	106
Cu^{2+}	$0.6_1 \pm 0.0_4$	2.0	$2.4_5 \pm 0.0_9$	92
		4.0	$4.5_1 \pm 0.1_5$	98
Pb^{2+}	<LOQ	2.0	$2.0_9 \pm 0.1_6$	105
		4.0	$4.3_6 \pm 0.2_7$	109

[a]Results obtained are attributed to the final diluted samples.

Table 3. Comparison of Extraction Recoveries (ER) and Maximum Adsorption Capacities (Q_m) of TMU-4, TMU-5, and TMU-6 for the Target Metal Ions

	TMU-4		TMU-5		TMU-6	
target metal ion	ER	Q_m (mg g^{-1})	ER	Q_m (mg g^{-1})	ER	Q_m (mg g^{-1})
Cd^{2+}	23	48	21	43	10	41
Co^{2+}	9.5	55	10	63	4	59
Cr^{3+}	53	127	54	123	7	118
Cu^{2+}	54	62	56	57	9	60
Pb^{2+}	36	237	35	251	18	224

DOI: 10.1021/ic5015384
Inorg. Chem. 2015, 54, 425−433

Table 4. Comparison of Maximum Adsorption Capacities (Q_m), Preconcentration Factors (PF), and Limits of Detection (LOD) of Some Sorbents Reported in the Literature for the Removal and Preconcentration of Target Metal Ions

sorbent	parameter	target metal ion Cd^{2+}	Co^{2+}	Cr^{3+}	Cu^{2+}	Pb^{2+}	ref
nanoalumina modified with 2,4-dinitrophenylhydrazine	Q_m (mg g^{-1})	83.33	41.66	100.0	–	100.00	48
Fe_3O_4 nanoparticles–poly(L-cysteine/2-hydroxyethyl acrylate)	Q_m (mg g^{-1})	27.55	–	5.98	15.72	39.06	49
Ca(II)-imprinted chitosan microspheres	Q_m (mg g^{-1})	50.89	–	–	54.76	78.92	50
xanthate-modified magnetic chitosan	Q_m (mg g^{-1})	–	–	–	65	76.9	51
multiwalled carbon nanotubes	Q_m (mg g^{-1})	10.86	–	–	–	97.08	52
silica-supported dithiocarbamate	Q_m (mg g^{-1})	40.3	–	–	–	70.4	53
nano-ZrO_2/B_2O_3	Q_m (mg g^{-1})	109.9	32.2	–	46.5	–	54
	PF	15	10	–	10	–	
	LOD (μg L^{-1})	3.1	3.8	–	3.3	–	
magnetic nanoparticles/bismuthiol II	Q_m (mg g^{-1})	–	–	8.6	5.3	9.4	55
	PF	–	–	96	95	87	
	LOD (μg L^{-1})	–	–	0.043	0.058	0.085	
iminodiacetic acid functionalized multiwalled carbon nanotubes	Q_m (mg g^{-1})	6.61	6.72	–	6.64	8.98	56
	PF	79	92	–	101	91	
	LOD (ng L^{-1})	0.79	0.4	–	2.5	0.7	
magnetic nanoparticles coated with 3-(trimethoxysilyl)-1-propantiol and modified with 2-amino-5-mercapto-1,3,4-thiadiazole	Q_m (mg g^{-1})	4.7	–	–	3.8	–	57
	PF	190	–	–	170	–	
	LOD (μg L^{-1})	0.12	–	–	0.13	–	
nanometer-sized alumina	Q_m (mg g^{-1})	17.7	9.5	13.6	13.3	17.5	58
	PF	5	5	5	5	5	
	LOD (μg L^{-1})	0.079	0.008	0.015	0.045	0.027	
zinc(II) metal–organic framework (TMU-5)	Q_m (mg g^{-1})	43	63	123	57	251	this work
	PF	81	42	216	225	137	
	LOD (μg L^{-1})	0.1	0.1	0.01	0.02	0.5	

adsorption of metal ions and that the main role is related to free sites on the MOF for interactions with metal ions and the basicity of the N-donor group in the MOF structure. Indeed, in TMU-6, two nitrogen atoms are in resonance with the benzene ring, which reduces their charge density and. therefore, their basicity.[46,47] In addition, because of the presence of a space between the two nitrogen atoms, they are less accessible for metal ions than the nitrogen atoms in the azine groups of TMU-5, and so, they have less interaction with metal ions. Based on these findings, the extraction efficiency of TMU-5 was greater than that of TMU-6. The results from comparison of the extraction efficiencies of the three MOFs showed that the adsorption mechanism is probably based on the interaction of the metal cations with the Lewis base sites of the MOFs, such as free nitrogens and oxygens (ether groups) based on Lewis acid–base interactions. However, the ether groups probably play an important role in the adsorption of metal ions in all three MOFs; because the ether linkages are similar in all three MOFs, they create identical conditions. Hence, they do not show different behaviors in metal ion adsorption. However, differences in the type of free nitrogen atoms in the three MOFs might result in different adsorption efficiencies.

To determine the role of the Lewis base sites of the MOFs in the adsorption of metal ions, far-IR (100–600 cm^{-1}) analysis of TMU-5 before and after exposure to Cr^{3+} ions was performed. Because metal bonding vibrations appear in the far-IR region, it was expected that additional peaks would be observed in the far-IR spectrum of TMU-5 after the adsorption of Cr^{3+} ions. As can be seen in Figure S6 (SI), there were some additional peaks in the IR spectrum of TMU-5 after the adsorption of metal ions. In spectrum b, denoted as TMU-5/Cr, some additional peaks in the range of 250–550 cm^{-1}, namely, 265, 300, 450, and 548 cm^{-1}, were observed that can be attributed to N–Cr and O–Cr interactions. According to these observed changes between two spectra (a and b), it can be concluded that interactions between the metal ions and the Lewis base sites (N or O) of the MOFs play a major role in the adsorption properties of the MOFs.

In addition, there is another piece of evidence regarding the role of Lewis base sites in the adsorption of the metal ions by

DOI: 10.1021/ic5015384
Inorg. Chem. 2015, 54, 425–433

the three MOFs. Because increasing the sample pH from 3 to 10 resulted in an enhancement of the adsorption efficiency of the metal ions on the MOFs, it can be concluded that the donor atoms of the MOFs (N or O) play some role in the adsorption process. Indeed, MOF donor atoms protonated at low pH values can be deprotonated by increasing the pH, so that they become free for the adsorption of metal ions.

To evaluate the adsorption capacities of the three MOFs, metal ion concentrations of 30−100 mg L^{-1} were investigated. Because high concentrations of metal ions at high pH values precipitate in hydroxide form, these investigations were performed at pH 6. Based on the obtained results in Table 3, it can be seen that there is no significant difference in the adsorption capacities of the three MOFs.

According to these results and the results in terms of the extraction efficiencies of the three MOFs at pH 10, it can be concluded that, for trace amounts of metal ions (at pH 10), the adsorption of metal ions occurs on the basis of interactions with free donor sites of the MOF and the MOF which has more basicity shows more adsorption efficiency, whereas at high concentrations of metal ions (at pH 6), void spaces in the MOFs play the main role in the adsorption process. Because all of the MOFs have similar void spaces, they showed almost the same adsorption capacity for metal ions.

Comparison of the maximum adsorption capacity (Q_m), preconcentration factor (PF) and limit of detection (LOD) of MOF TMU-5 with those of the other sorbents presented in literature for metal ions removal and extraction is listed in Table 4. As can be seen, the characteristics of the proposed MOF sorbent are better than, or at least comparable to, those of other sorbents reported for the removal and extraction of heavy-metal ions. In particular, TMU-5 has a very higher adsorption capacity for the toxic heavy metal of Pb. These findings illustrate that our MOF has a high porosity and surface area and can be accepted as new class of materials for adsorption applications.

CONCLUSIONS

In summary, this work reported an exploration of the Zn(II)-based MOFs TMU-4, TMU-5, and TMU-6 decorated with azine and imine groups with accessible Lewis basic sites for the adsorption and extraction of some heavy-metal ions. The obtained results revealed that TMU-5 has nearly the same extraction efficiency as TMU-4 for metal ions, whereas its extraction efficiency is much greater than that of TMU-6 because of the more efficient interaction of the azine groups in TMU-5 with metal ions as compared with nitrogen atoms in TMU-6. Also, comparison of the adsorption capacities of the three MOFs at pH 6 leads to about the same results for all MOFs. These results illustrate that, in the adsorption of metal ions at high concentrations (pH 6), the void spaces of the MOFs play a main role in adsorption processes. In this work, all three MOFs were prepared by mechanosynthesis as a convenient, rapid, low-cost, solventless, and green process, and sorbent synthesis occurred on a large scale with a high yield. PXRD patterns confirmed that TMU-4, TMU-5, and TMU-6 synthesized based on mechanosynthesis are structurally identical to those prepared by conventional heating reaction. Water stability tests illustrated that all three MOFs are stable in water even for long periods of time. Comparison of TMU-5 with other sorbents reported in the literature illustrated that this MOF has a better adsorption capacity than many other sorbents, especially the toxic heavy metal Pb. Some advantages of the proposed procedure for the extraction and preconcentration of target heavy-metal ions are the possibility of extraction from large volumes of samples in short extraction times because of the short diffusion route; low sorbent requirements (because of a high adsorption capacity); no application of organic chelating agents and organic solvents that are commonly used in the complexation and extraction of metal ions and, consequently, less organic waste; simplicity; and low cost. Remarkable water and wide pH range stability of the MOFs characterize the materials as being different from other moisture-sensitive MOFs, and therefore, makes them a more suitable sorbent for adsorption and extraction applications. These results offer promising applications for the new MOFs as efficient sorbents for the extraction and preconcentration of heavy-metal ions from water samples.

ASSOCIATED CONTENT

Supporting Information

FE-SEM images (Figure S1), N_2 isotherm at 77 K and 1 bar of mechanosynthesized TMU-6 (Figure S2), thermogravimetric profiles (Figure S3), effect of extraction time (Figure S4), effect of eluent volume (Figure S5), ICP-OES operating conditions (Table S1), and tolerance limit of interfering foreign ions (Table S2). This material is available free of charge via the Internet at http://pubs.acs.org.

AUTHOR INFORMATION

Corresponding Author

*E-mail: morsali_a@modares.ac.ir. Tel.: +98-21-82883449.

Author Contributions

†E.T. and M.Y.M. contributed equally to this work.

Notes

The authors declare no competing financial interest.

ACKNOWLEDGMENTS

Support of this investigation by Tarbiat Modares University is gratefully acknowledged.

REFERENCES

(1) Yaghi, O. M.; O'Keeffe, M.; Ockwig, N. W.; Chae, H. K.; Eddaoudi, M.; Kim, J. *Nature* **2003**, *423*, 705−714.
(2) Eddaoudi, M.; Kim, J.; Rosi, N.; Vodak, D.; Wachter, J.; O'Keeffe, M.; Yaghi, O. M. *Science* **2002**, *295*, 469−472.
(3) Chen, B.; Xiang, S.; Qian, G. *Acc. Chem. Res.* **2010**, *43*, 1115−1124.
(4) Ravikumar, I.; Ghosh, P. *Chem. Soc. Rev.* **2012**, *41*, 3077−3098.
(5) Li, J.-R.; Kuppler, R. J.; Zhou, H.-C. *Chem. Soc. Rev.* **2009**, *38*, 1477−1504.
(6) Cychosz, K. A.; Ahmad, R.; Matzger, A. J. *Chem. Sci.* **2010**, *1*, 293−302.
(7) Li, J.-R.; Sculley, J.; Zhou, H.-C. *Chem. Rev.* **2011**, *112*, 869−932.
(8) Suh, M. P.; Park, H. J.; Prasad, T. K.; Lim, D.-W. *Chem. Rev.* **2011**, *112*, 782−835.
(9) Zhao, Y.; Seredych, M.; Zhong, Q.; Bandosz, T. J. *ACS Appl. Mater. Interfaces* **2013**, *5*, 4951−4959.
(10) Li, J.-R.; Ma, Y.; McCarthy, M. C.; Sculley, J.; Yu, J.; Jeong, H.-K.; Balbuena, P. B.; Zhou, H.-C. *Coord. Chem. Rev.* **2011**, *255*, 1791−1823.
(11) Kreno, L. E.; Leong, K.; Farha, O. K.; Allendorf, M.; Van Duyne, R. P.; Hupp, J. T. *Chem. Rev.* **2011**, *112*, 1105−1125.
(12) Horcajada, P.; Serre, C.; Vallet-Regí, M.; Sebban, M.; Taulelle, F.; Férey, G. *Angew. Chem.* **2006**, *118*, 6120−6124.

DOI: 10.1021/ic5015384
Inorg. Chem. 2015, 54, 425−433

(13) Horcajada, P.; Gref, R.; Baati, T.; Allan, P. K.; Maurin, G.; Couvreur, P.; Férey, G.; Morris, R. E.; Serre, C. *Chem. Rev.* **2011**, *112*, 1232−1268.
(14) Della Rocca, J.; Liu, D.; Lin, W. *Acc. Chem. Res.* **2011**, *44*, 957−968.
(15) Masoomi, M. Y.; Morsali, A. *Coord. Chem. Rev.* **2012**, *256*, 2921−2943.
(16) Wang, Z.; Chen, G.; Ding, K. *Chem. Rev.* **2008**, *109*, 322−359.
(17) Ma, L.; Abney, C.; Lin, W. *Chem. Soc. Rev.* **2009**, *38*, 1248−1256.
(18) Gu, Z.-Y.; Yang, C.-X.; Chang, N.; Yan, X.-P. *Acc. Chem. Res.* **2012**, *45*, 734−745.
(19) Ni, Z.; Jerrell, J. P.; Cadwallader, K. R.; Masel, R. I. *Anal. Chem.* **2007**, *79*, 1290−1293.
(20) Gu, Z.-Y.; Wang, G.; Yan, X.-P. *Anal. Chem.* **2010**, *82*, 1365−1370.
(21) Chen, X.; Ding, N.; Zang, H.; Yeung, H.; Zhao, R.-S.; Cheng, C.; Liu, J.; Chan, T. W. D. *J. Chromatogr. A* **2013**, *1304*, 241−245.
(22) Gu, Z.-Y.; Chen, Y.-J.; Jiang, J.-Q.; Yan, X.-P. *Chem. Commun.* **2011**, *47*, 4787−4789.
(23) Chen, X.-F.; Zang, H.; Wang, X.; Cheng, J.-G.; Zhao, R.-S.; Cheng, C.-G.; Lu, X.-Q. *Analyst* **2012**, *137*, 5411−5419.
(24) Cui, X.-Y.; Gu, Z.-Y.; Jiang, D.-Q.; Li, Y.; Wang, H.-F.; Yan, X.-P. *Anal. Chem.* **2009**, *81*, 9771−9777.
(25) Chang, N.; Gu, Z.-Y.; Wang, H.-F.; Yan, X.-P. *Anal. Chem.* **2011**, *83*, 7094−7101.
(26) Chen, B.; Liang, C.; Yang, J.; Contreras, D. S.; Clancy, Y. L.; Lobkovsky, E. B.; Yaghi, O. M.; Dai, S. *Angew. Chem., Int. Ed.* **2006**, *45*, 1390−1393.
(27) Gu, Z.-Y.; Yan, X.-P. *Angew. Chem., Int. Ed.* **2010**, *49*, 1477−1480.
(28) Gu, Z.-Y.; Jiang, J.-Q.; Yan, X.-P. *Anal. Chem.* **2011**, *83*, 5093−5100.
(29) Xie, S.-M.; Zhang, Z.-J.; Wang, Z.-Y.; Yuan, L.-M. *J. Am. Chem. Soc.* **2011**, *133*, 11892−11895.
(30) Gu, Z.-Y.; Jiang, D.-Q.; Wang, H.-F.; Cui, X.-Y.; Yan, X.-P. *J. Phys. Chem. C* **2009**, *114*, 311−316.
(31) Ameloot, R.; Liekens, A.; Alaerts, L.; Maes, M.; Galarneau, A.; Coq, B.; Desmet, G.; Sels, B. F.; Denayer, J. F. M.; De Vos, D. E. *Eur. J. Inorg. Chem.* **2010**, *2010*, 3735−3738.
(32) Yang, C.-X.; Liu, S.-S.; Wang, H.-F.; Wang, S.-W.; Yan, X.-P. *Analyst* **2012**, *137*, 133−139.
(33) Yang, C.-X.; Yan, X.-P. *Anal. Chem.* **2011**, *83*, 7144−7150.
(34) Ahmad, R.; Wong-Foy, A. G.; Matzger, A. J. *Langmuir* **2009**, *25*, 11977−11979.
(35) Alaerts, L.; Kirschhock, C. E. A.; Maes, M.; vanderVeen, M. A.; Finsy, V.; Depla, A.; Martens, J. A.; Baron, G. V.; Jacobs, P. A.; Denayer, J. F. M.; DeVos, D. E. *Angew. Chem., Int. Ed.* **2007**, *46*, 4293−4297.
(36) Nuzhdin, A. L.; Dybtsev, D. N.; Bryliakov, K. P.; Talsi, E. P.; Fedin, V. P. *J. Am. Chem. Soc.* **2007**, *129*, 12958−12959.
(37) Gerhardsson, L.; Skerfving, S. *Toxicology of Metals*; CRC Press: Boca Raton, FL, 1996; Vol. *I*.
(38) Wu, Y.; Hu, B.; Jiang, Z.; Feng, Y.; Lu, P.; Li, B. *Rapid Commun. Mass Spectrom.* **2006**, *20*, 3527−3534.
(39) Akatsuka, K.; McLaren, J. W.; Lam, J. W.; Berman, S. S. *J. Anal. At. Spectrom.* **1992**, *7*, 889−894.
(40) Daftsis, E. J.; Zachariadis, G. A. *Talanta* **2007**, *71*, 722−730.
(41) Simpson, N. J. K., Ed. *Solid-Phase Extraction: Principles, Techniques, and Applications*; Marcel Dekker: New York, 2000.
(42) Masoomi, M. Y.; Stylianou, K. C.; Morsali, A.; Retailleau, P.; Maspoch, D. *Cryst. Growth Des.* **2014**, *14*, 2092−2096.
(43) Masoomi, M. Y.; Beheshti, S.; Morsali, A. *J. Mater. Chem. A* **2014**, *2*, 16863−16866.
(44) Ciurtin, D. M.; Dong, Y.-B.; Smith, M. D.; Barclay, T.; zur Loye, H.-C. *Inorg. Chem.* **2001**, *40*, 2825−2834.
(45) Spek, A. L. *J. Appl. Crystallogr.* **2003**, *36*, 7−13.
(46) Carey, F. A., Sundberg, R. J. *Advanced Organic Chemistry*; Springer: New York, 2007.
(47) Edwards, J. O.; Pearson, R. G. *J. Am. Chem. Soc.* **1962**, *84*, 16−24.
(48) Afkhami, A.; Saber-Tehrani, M.; Bagheri, H. *J. Hazard. Mater.* **2010**, *181*, 836−844.
(49) Hua, R.; Li, Z. *Chem. Eng. J.* **2014**, *249*, 189−200.
(50) He, J.; Lu, Y.; Luo, G. *Chem. Eng. J.* **2014**, *244*, 202−208.
(51) Zhu, Y.; Hu, J.; Wang, J. *J. Hazard. Mater.* **2012**, *221−222*, 155−161.
(52) Li, Y.-H.; Ding, J.; Luan, Z.; Di, Z.; Zhu, Y.; Xu, C.; Wu, D.; Wei, B. *Carbon* **2003**, *41*, 2787−2792.
(53) Bai, L.; Hu, H.; Fu, W.; Wan, J.; Cheng, X.; Zhuge, L.; Xiong, L.; Chen, Q. *J. Hazard. Mater.* **2011**, *195*, 261−275.
(54) Yalçınkaya, Ö.; Kalfa, O. M.; Türker, A. R. *J. Hazard. Mater.* **2011**, *195*, 332−339.
(55) Suleiman, J. S.; Hu, B.; Peng, H.; Huang, C. *Talanta* **2009**, *77*, 1579−1583.
(56) Wang, J.; Ma, X.; Fang, G.; Pan, M.; Ye, X.; Wang, S. *J. Hazard. Mater.* **2011**, *186*, 1985−1992.
(57) Mashhadizadeh, M. H.; Karami, Z. *J. Hazard. Mater.* **2011**, *190*, 1023−1029.
(58) Yin, J.; Jiang, Z.; Chang, G.; Hu, B. *Anal. Chim. Acta* **2005**, *540*, 333−339.

DOI: 10.1021/ic5015384
Inorg. Chem. 2015, 54, 425−433